




Maghemite Nanoparticles for DNA Extraction: Performance and Blocking Temperature

S. V. Stolyar^{1,2,3} · S. V. Komogortsev² · A. S. Gorbenko¹ · Yu. V. Knyazev² · R. N. Yaroslavtsev^{1,2}  · I. A. Olkhovskiy¹ · D. S. Neznakhin⁴ · A. V. Tyumentseva¹ · O. A. Bayukov² · R. S. Iskhakov²

Received: 10 May 2021 / Accepted: 25 March 2022 / Published online: 29 April 2022
© The Author(s), under exclusive licence to Springer Science+Business Media, LLC, part of Springer Nature 2022

Abstract

Iron oxide nanoparticles coated with polyethylene glycol were synthesized by coprecipitation for use in the magnetic separation of DNA (deoxyribonucleic acid). The blocking temperature of nanoparticles was studied by the methods of Mössbauer spectroscopy, ferromagnetic resonance, and using magnetometric measurements. The blocking temperature calculated from the temperature dependence of the coercive force was ~200 K. The calculation of the blocking temperature from the relaxation time obtained using Mössbauer spectroscopy gave a value of ~450 K. The blocking temperature obtained using ferromagnetic resonance was ~910 K. The relationship between the obtained blocking temperatures is in good agreement with the Néel-Brown formula. The constants of effective and surface anisotropy were determined by the method of ferromagnetic resonance. Isolation of DNA from blood using prepared particles and separation in a permanent magnet field revealed sufficient productivity, high speed, and the “chemical delicacy” of this approach.

Keywords Magnetic nanoparticles · Superparamagnetism · Blocking temperature · Magnetic separation

1 Introduction

DNA separation is one of the important areas of biomedicine, relevant both for the clinical diagnosis of diseases and, in some cases, for monitoring their course [1, 2]. Compared to the currently used sorption methods, the use of magnetic nanoparticles for DNA isolation has some advantages, including a reduction in the isolation time due to the replacement of the sample centrifugation procedure with short-term exposure to a magnetic field, as well as the possibility of automating the isolation process, which is especially important for large flows of molecular genetic research [3–5]. There are already known examples of the use of magnetic nanoparticles of iron oxides with a modified surface for selective sorption and isolation of certain biomolecules,

such as nucleic acids and proteins [1, 2, 6]. Research into new compositions of nanoparticles is underway, and equipment for the automation of separation is being developed [7, 8].

For many biomedical applications, and in particular, for the separation of biomolecules, magnetic nanoparticles are used in the form of colloidal solutions [9–11]. An important problem is the instability of colloids, one of the reasons for which is the magnetic dipole–dipole interaction between particles. The movement of magnetic particles using an external inhomogeneous magnetic field requires a high magnetic susceptibility of colloid particles [12]. These properties of nanoparticles differ significantly depending on the stability of the orientation of their magnetic moment to the action of thermal fluctuations. The use of superparamagnetic particles exhibiting thermally stimulated magnetization reversal, hysteresisless behavior, and having a smaller size contributes to better colloidal stability of the ensemble. Particles, the magnetic moment of which is thermally stable, that is, in a blocked state, are more susceptible to weak external fields. The key parameter that determines the state of the particles is the blocking temperature, above which the particles are superparamagnetic and below which their magnetic moment is blocked. The use of particles with a blocking temperature close to the ambient temperature for magnetic separation is an optimal compromise combining

✉ R. N. Yaroslavtsev
yar-man@bk.ru

¹ Krasnoyarsk Scientific Center, Federal Research Center KSC SB RAS, Krasnoyarsk, Russia

² Kirensky Institute of Physics, Federal Research Center KSC SB RAS, Krasnoyarsk, Russia

³ Siberian Federal University, Krasnoyarsk, Russia

⁴ Ural Federal University, Ekaterinburg, Russia

colloid stability and high magnetic susceptibility. Therefore, the preparation of new particles requires control of their blocking temperature. The blocking temperature depends on the characteristic measurement time (for characterization) or the time the particle performs a certain function (in applications). For example, in measurements in low-frequency (including constant) magnetic fields, the characteristic measurement time is $\sim 10^{-2} \div 10^2$ s, in ferromagnetic resonance $\sim 10^{-10}$ s, and in Mössbauer spectroscopy $\sim 2.5 \cdot 10^{-8}$ s. The shorter the characteristic time, the higher the blocking temperature obtained in the corresponding experiment [13]. Therefore, the method for determining the blocking temperature must be selected depending on the specific practical application of nanoparticles. If nanoparticles are used in a constant magnetic field (for example, magnetic separation), then magnetometric measurements should be used to determine the blocking temperature, and if in alternating fields with high frequencies, then Mössbauer spectroscopy or ferromagnetic resonance.

This work aimed to obtain and comprehensively characterize magnetic nanocomposite particles based on γ - Fe_2O_3 for the efficient separation of DNA molecules from blood cells. Since the chemical interaction of DNA with the surface of new nanocomposite particles can lead to undesirable chemical effects (in particular, oxidative damage to DNA), control of the quantity and quality of DNA isolated from blood was also an important part of the work.

2 Experiment

For the synthesis of iron oxide nanoparticles, the coprecipitation method was used, in which nanoparticles are formed from water-salt solutions by adding alkali at room

temperature. Complete precipitation occurs at pH values in the range from 8 to 14. The shape and composition of the particles depend on the type of salt (chlorides, sulfates, nitrates), the $\text{Fe}^{2+}/\text{Fe}^{3+}$ ratio, the reaction temperature, pH, the type of alkali, and the stirring speed.

In this work, magnetic nanoparticles were prepared using salts of iron chloride (II) and (III) and an aqueous solution of ammonia. At room temperature, 2.75 g $\text{FeCl}_3 \cdot 4\text{H}_2\text{O}$ and 1.01 g $\text{FeCl}_2 \cdot 6\text{H}_2\text{O}$ were dissolved in 50 ml of distilled water with magnetic stirring. Three milliliters of NH_4OH (25%) was added dropwise to the iron salts mixture with constant stirring. Stirring was continued for 4 h. At the end of the reaction, the magnetic sediment was washed several times in distilled water to pH = 7.0. To use the nanoparticles for DNA separation, they were previously treated with an aqueous solution 1.25 M sodium chloride and 10% polyethylene glycol (PEG 6000).

Electron microscopic studies were carried out on a Hitachi HT7700 transmission electron microscope (accelerating voltage 100 kV) of the Krasnoyarsk Regional Center of Research Equipment of Federal Research Center “Krasnoyarsk Science Center SB RAS.” The Mössbauer spectra were measured on an MS-1104Em spectrometer with a $^{57}\text{Co}(\text{Rh})$ source at room temperature. Isomeric chemical shifts are indicated relative to α -Fe. The magnetic properties were studied on an MPMS XL7 SQUID magnetometer, Quantum Design. Ferromagnetic resonance (FMR) spectra were measured with the X-band (9.7 GHz) spectrometer ELEXSYS E580 (Bruker, Germany).

The study of the ability of nanoparticles to adsorb nucleic acids was carried out as follows. Leukocyte lysate from a blood sample obtained from a voluntary donor was added to the nanoparticle suspension. Then, the nanoparticles

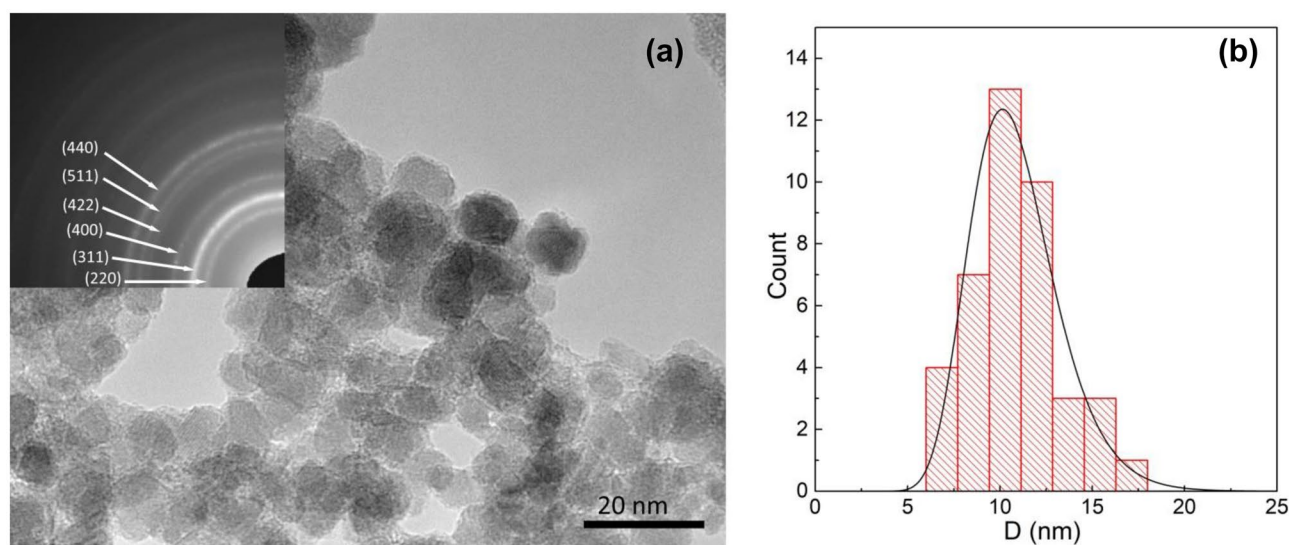


Fig. 1 TEM image of iron oxide nanoparticles (a), diffraction pattern (inset), and size distribution (b)

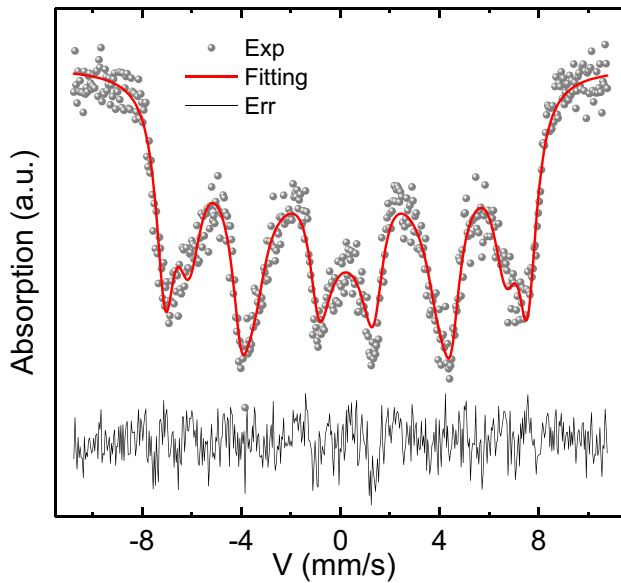


Fig. 2 Mössbauer spectrum of the sample

bound to DNA molecules were separated using a magnet. Subsequent washing of DNA from nanoparticles was performed with ethanol at room temperature, then elution was performed in TE buffer. The resulting eluate was subjected to a real-time PCR (polymerase chain reaction) to detect the JAK2 gene. As a comparison, a reaction was performed with DNA samples isolated by the sorption method using a commercial kit “DNA-Sorb-B” (Amplisens, Russia).

3 Results

According to TEM (transmission electron microscopy) images (Fig. 1a), the nanoparticles have a spherical shape with an average size of 10.9 nm. Figure 1b shows the particle size distribution. The inset in Fig. 1a shows a diffraction pattern in which the positions of all recorded rings correspond to γ -Fe₂O₃ maghemite.

The Mössbauer spectrum of the sample and the processing result are shown in Fig. 2. The error is shown below the spectrum, i.e., difference between calculated and

experimental spectra. Spectrum processing was carried out based on the relaxation two-level model proposed in the works [14, 15]. Since electron microscopy results indicate rather small particle sizes, it can be assumed that the broadening of the spectral lines is a consequence of the closeness of the relaxation time of the magnetic moment of the particles to the characteristic measurement time. The spectrum is approximated by the sum of three sextets. The presence of several sextets can be explained by the particle size distribution, which leads to a certain spread in the relaxation times of their magnetic moments. Mössbauer parameters are given in Table 1.

For magnetic characterization of nanoparticles, we measured the magnetization curves at different temperatures (Fig. 3) and the temperature behavior of the magnetization according to the ZFC–FC (zero-field-cooled and field-cooled) protocol in a field of 100 Oe (Fig. 4).

According to Fig. 4, the magnetic hysteresis in a field of 100 Oe, which determines the difference between the ZFC and FC curves, becomes vanishingly small at temperatures above 200 K. The value of the coercive force was calculated from the magnetization curves. As it turned out, the temperature behavior of the coercive force differs from the standard power dependence:

$$H_c(T) = H_c(0) \cdot \left(1 - \left(\frac{T}{T_B}\right)^\alpha\right). \quad (1)$$

Usually, the dependence of the form (1) is used to describe the behavior of single-domain non-interacting nanoparticles at temperatures below the blocking temperature (T_B) [16–18]. Power exponent α ranges from 0.67 to 1 [19–23]. The inhomogeneity of the blocking temperature in the system of the studied nanoparticles can be the reason for such a deviation. The blocking temperature inhomogeneity is due to the size distribution of nanoparticles and, in addition, to interparticle interactions.

Figure 5 shows the ferromagnetic resonance spectra of nanoparticles in the temperature range 110–370 K. With increasing temperature, the intensity of the absorption peak and the value of the resonance field increase, and the linewidth decreases (Fig. 6).

Table 1 Results of processing the Mössbauer spectrum

IS, mm/s ± 0.005	$\langle H_{hf} \rangle$, kOe, ± 3	QS, mm/s ± 0.01	τ_0 , s	A, % ± 2.0	Position
0.505	297	−0.08	9.8E-9	0.35	S1
0.387	398	0.07	2.4E-8	0.33	S2
0.360	456	0.01	3.4E-8	0.32	S3

IS is the isomeric shift relative to α -Fe, $\langle H_{hf} \rangle$ is the hyperfine field at the iron core, QS is the quadrupole splitting, τ_0 is the relaxation time, and A is the occupancy of the iron positions

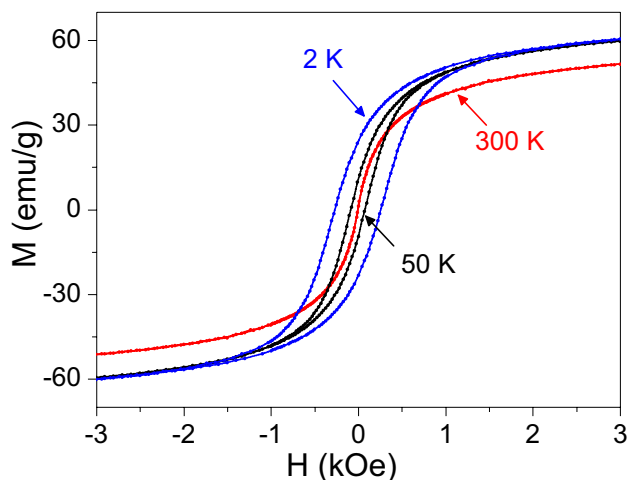


Fig. 3 Magnetization curves measured at temperatures of 2 K (blue line), 50 K (black line), and 300 K (red line) in the applied field from -3 to 3 kOe

Isolation of DNA using the developed magnetic nanoparticles in comparison with the standard method of sorption on silica showed that the amount of DNA isolated was 15.4 ng with standard isolation and 75 ng with isolation using magnetic nanoparticles. RT-PCR demonstrated the absence of inhibitory components in the mixture. This indicates the purity of the DNA obtained using magnetic nanoparticles and the absence of their influence on the quality of the isolated molecules.

4 Discussion

Relaxation processes in magnetic nanoparticles proceed faster than the lifetime of the excited state of ^{57}Fe nuclei ($2.5 \cdot 10^{-8}$ s). Therefore, the effective state of the magnetic

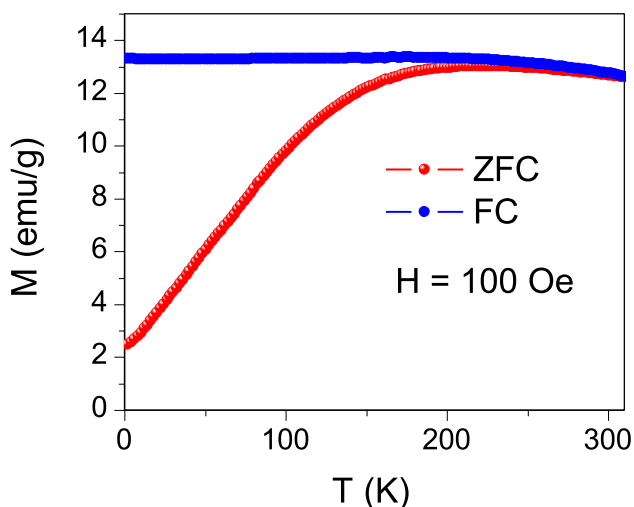


Fig. 4 Temperature behavior of magnetization in a field of 100 Oe measured according to the ZFC–FC protocol

moment of the particle averaged over the lifetime of the excited state of ^{57}Fe nuclei can be observed by the method of Mössbauer spectroscopy. Therefore, the table contains the values of $\langle H_{\text{hf}} \rangle$, which indicate that some of the magnetic nanoparticles (S1) have a relaxation time close to the temperature of the spectrum set (300 K). This is also indicated by the calculated relaxation time τ_0 . The other two components of the spectrum in the considered model have long relaxation times, which can be regarded as a blocked state of the particle's magnetic moment. The decreased value of the S2 hyperfine field is possibly related to the nanoparticles' defectiveness (cation vacancies).

Within the framework of the used model [14, 15], we can divide all particles into two groups: (1) with a blocked magnetic moment at 300 K (S2 and S3 sextets) and (2) with an unblocked magnetic moment at 300 K (S1 sextet). According to the data in Table 1, the S3 sextet has the closest hyperfine parameters to bulk maghemite. In addition, the calculated relaxation time of the magnetic moment for the S3 sextet is longer than the characteristic measurement time of Mössbauer spectroscopy (τ), so we can assume that this sextet describes the behavior of blocked nanoparticles, whereas for sextet S1, the relaxation time is significantly less than τ , that is, S1 sextet refers to unblocked particles, and for sextet S2, the relation $\tau_0 \approx \tau$ is fulfilled. Taking into account the histogram of particle size distribution obtained from HRTEM data, we can say that particles smaller than 9.5 nm (about 30%, which corresponds to the spectral fraction S3) are in an unblocked state, while particles 10 – 18 nm in size are in a blocked state [24]. If we assume that the critical size of nanoparticles with a blocking temperature of 300 K is 9.5 nm in diameter, then the average blocking temperature of nanoparticles can be estimated using the Néel-Brown formula [25]:

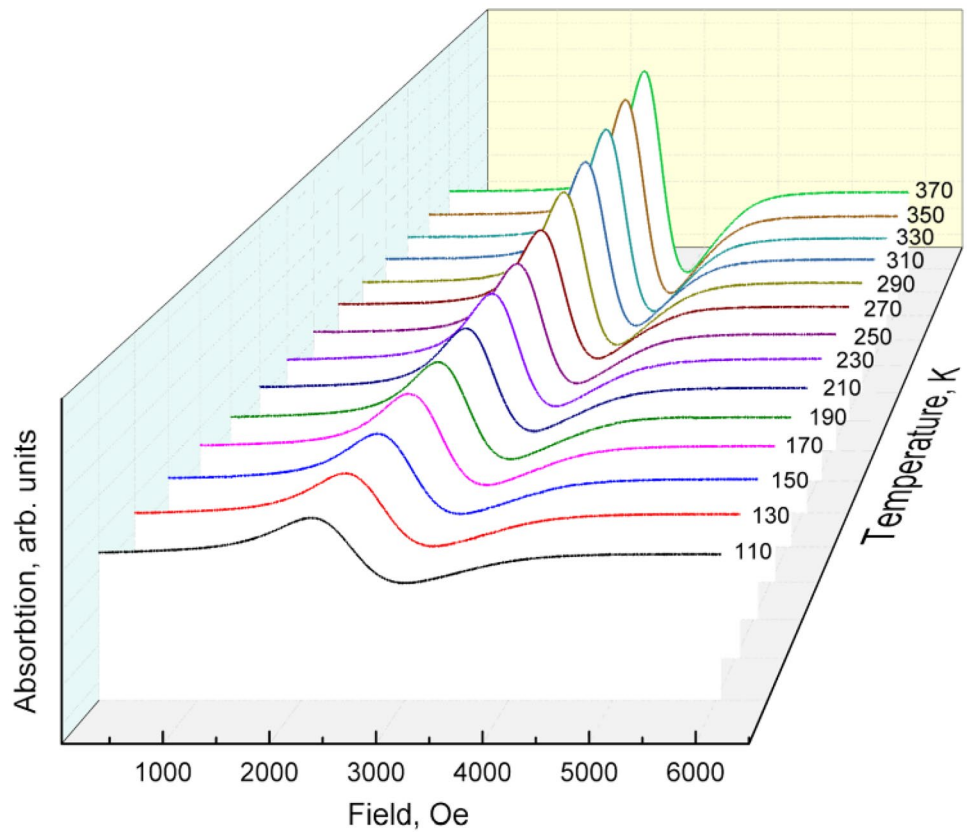
$$\ln\left(\frac{\tau}{\tau_0}\right) = \frac{k_B T}{K_{\text{eff}} V_{\text{crit}}}, \quad (2)$$

where K_{eff} is the effective anisotropy constant, V is the volume of a spherical particle, and $\tau \approx 1/\nu_L$ is the characteristic measurement time, where ν_L is the Larmor frequency for iron nuclei in the sample determined by the expression $\nu_L = H\mu_1/\hbar = 4.7 \cdot 10^7 \text{ s}^{-1}$.

Assuming that the anisotropy constant of maghemite nanoparticles varies slightly within the observed distribution, and the average nanoparticle size according to HRTEM data is 10.9 nm, then the estimated value of the average blocking temperature for the sample is

$$T_B = T_B^{9.5\text{nm}} \frac{\langle V_{\text{crit}} \rangle}{V_{\text{crit}}^{300}} = 300 \frac{10.9^3}{9.5^3} = 450 \text{ K}. \quad (3)$$

Fig. 5 Ferromagnetic resonance spectra measured in the temperature range of 110–370 K



Particle size and magnetic anisotropy distributions can lead to inhomogeneity of the blocking temperature in the ensemble of particles. To quantify this inhomogeneity (blocking temperature distribution), we analyzed the data in Figs. 3 and 4 using different methods.

To describe the coercive force, we used the following expression [17]:

$$\langle H_c(T) \rangle = \langle H_c(0) \rangle \cdot \frac{\int H_c(T) f(T_B) dT_B}{\int f(T_B) dT_B}, \tag{4}$$

where $\langle H_c(0) \rangle$ parameter is the average coercive force at $T=0$ K. We fitted the experimental behavior of the coercive force by expression (4) and determined the parameters of the distribution function $f(T_B)$ corresponding to the best description of the experiment. The best agreement is achieved using the lognormal distribution function:

$$f(T_B) = \frac{1}{T_B \cdot \sigma \sqrt{2\pi}} \cdot \exp\left(-\ln^2\left(\frac{T_B}{T_{B0}}\right)/2\sigma^2\right) \text{ with the parameters } T_{B0} = 90 \text{ K}, \sigma = 77$$

Another approach to assessing the blocking temperature is to use the graph measured using the ZFC–FC protocol (Fig. 4). The use of these data makes it possible to estimate the distribution of particles over the blocking temperature as [26–28]:

$$\tilde{f}(T_B) = -\frac{\Delta(M_{FC}(T) - M_{ZFC}(T))}{\Delta T} \tag{5}$$

The distribution estimated by this method deviates slightly from the lognormal distribution using the parameters corresponding to the best fitting for the temperature behavior of the H_c in Eq. (4) (Fig. 7). This discrepancy may be the result of dipole–dipole interaction in the particle system. Note that Fig. 7 shows the number-weighted distributions. For practice, the volume-weighted distribution of particles is more important. The estimate of the volumetric average blocking temperature is $\langle T_B \rangle_V = 200 \pm 20$ K. This value is in good agreement with the temperature at which the difference between the ZFC and FC curves becomes vanishingly small.

Taking into account that the width of the distribution of particles over the blocking temperature is quite large (see Fig. 7), it can be concluded that a significant fraction of

particles has blocking temperatures close to the operating temperatures (~ 300 K).

To analyze the measurements of ferromagnetic resonance, we used the theory [29, 30], which assumes that

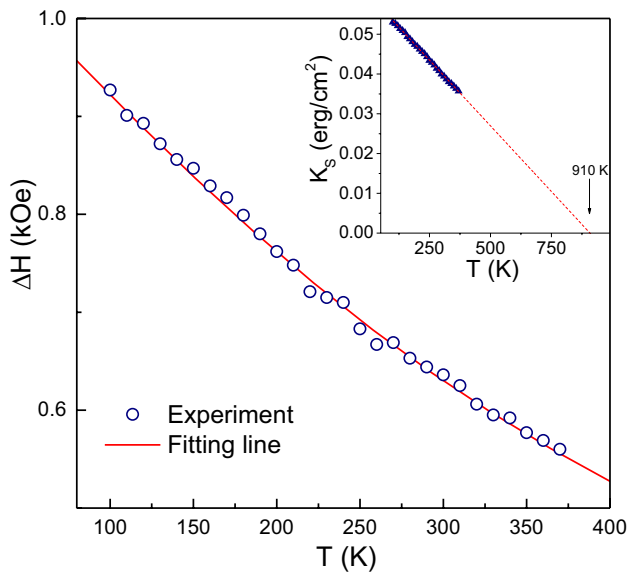


Fig. 6 Dependence of the FMR line width on temperature. Inset: temperature dependence of surface anisotropy K_s calculated from Eq. (7)

for a system of randomly oriented ferromagnetic particles, the FMR linewidth is the sum of two contributions ($\Delta H(T) = \Delta H_S(T) + \Delta H_U(T)$): broadening due to superparamagnetism of nanoparticles ($\Delta H_S(T)$) and broadening due to the dispersion of the directions of the anisotropy fields of particles ($\Delta H_U(T)$):

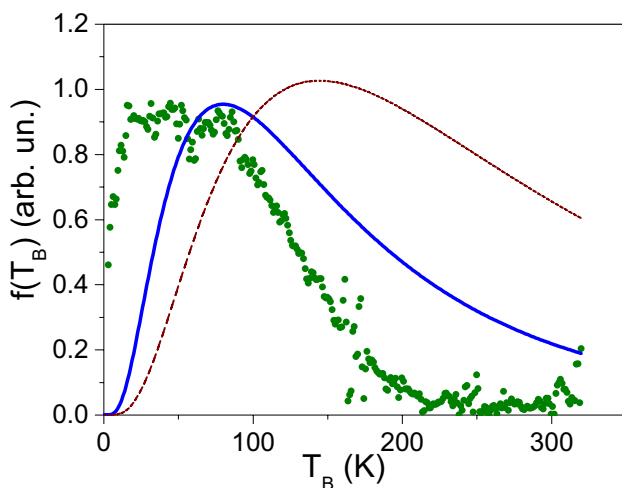


Fig. 7 Blocking temperature distribution estimated by different methods. Symbols, estimation from ZFC–FC according to formula (5); solid blue line, lognormal distribution with parameters corresponding to the best fitting of temperature behavior H_c by Eq. (4); dashed cherry line, volume-weighted distribution density recalculated from the lognormal distribution

$$\Delta H_S(T) = \frac{2}{\sqrt{3}} \frac{\omega}{\gamma} \frac{\alpha(x - L_1)}{xL_1} \quad \text{and} \quad \Delta H_U(T) = 3 \frac{\omega}{\gamma} \frac{\varepsilon L_2}{L_1}, \quad (6)$$

where $\alpha = 0.01$ is the attenuation parameter, $\varepsilon = K\gamma/M\omega$, K is the anisotropy constant, and $L_{1,2}$ is the Langevin functions. $\Delta H_S(T)$ and $\Delta H_U(T)$ are functions of the Langevin parameter $x = \frac{\omega}{\gamma} \frac{MV}{kT}$, where M is the magnetization, V is the particle volume, k is the Boltzmann constant, T is the temperature, ω is the frequency, and γ is the gyromagnetic ratio.

Figure 6 shows the values of the FMR linewidth of nanoparticles depending on temperature and the result of fitting the experimental data. The linewidth was determined from the distance between the left and right peaks of the differential absorption curve (peak-to-peak linewidth). The fitting curve shown in Fig. 6 is characterized by two fitting parameters: $K_{eff}V = 5.75 \cdot 10^{-14}$ erg and $MV = 4.7 \cdot 10^{-17}$ emu. Assuming that the magnetization of nanoparticles is 300 G, the nanoparticle size and anisotropy constant can be calculated. Thus, the size is 6.7 nm and the anisotropy constant $K_{eff} = 3.65 \cdot 10^5$ erg/cm³. The deviation of the average size of nanoparticles from the TEM results can be explained by the fact that atoms of the surface disordered layer do not participate in ferromagnetic resonance.

The effective anisotropy constant determined from the FMR is in good agreement with the value $K_{eff} = 5.48 \times 10^5$ erg/cm³, which was calculated in [31] for maghemite nanoparticles with an average diameter of 7 nm.

The resonance field H_R of maghemite nanoparticles increases monotonically with increasing temperature (Fig. 5), and the value of the resonance field is lower than ω/γ , which for a given frequency is 3460 Oe. In other words, a temperature-dependent shift of the H_R is observed, which is associated with the presence of surface unidirectional anisotropy K_S in nanoparticles. The surface magnetic anisotropy is due to the difference in the symmetry of the environment of the surface atomic magnetic moments from the bulk ones. The K_S value can be estimated using the relation [32]:

$$6K_S/MD = \omega/\gamma - H_R, \quad (7)$$

where K_S is the surface anisotropy constant, M is the magnetization, and D is the particle diameter. The result of calculating the surface anisotropy is shown in the inset in Fig. 7. The obtained value of the surface anisotropy is in good agreement with the previously obtained data [33].

Apparently, the T_B^{FMR} value can be estimated from the temperature dependence of the surface anisotropy constant. In the superparamagnetic state, the anisotropy, including K_S , will no longer affect the position of the FMR line. Therefore, the temperature at which the $6K_S/MD$ value reaches zero can be considered the blocking temperature (Fig. 6 inset). This temperature (910 K) is close to the maghemite T_C (985 K).

The blocking temperatures estimated from magnetometric measurements, ferromagnetic resonance, and Mössbauer spectroscopy are in reasonable agreement with each other and satisfy the corollary from the Néel-Brown relationship:

$$T_B^{M(T)} \approx T_B^{MS}/2 \approx T_B^{FMR}/4.$$

Isolation of DNA from blood using magnetic particles and separation in a permanent magnet field has shown sufficient productivity, high isolation rate, and “chemical delicacy” of this approach. According to the PCR results, DNA isolation from human blood samples using magnetic nanoparticles does not affect the amplification efficiency.

5 Conclusions

PEG-coated maghemite nanoparticles were synthesized by coprecipitation. According to the results of electron microscopy and Mössbauer spectroscopy, the nanoparticles are maghemite with an average size of ~10.9 nm. The values of magnetization, coercive force, blocking temperature, and effective and surface anisotropy constants are determined. Besides, using Mössbauer spectroscopy, the average blocking temperature was estimated, which was 450 K. The blocking temperature was also estimated from measurements of ferromagnetic resonance, which was 420 K. The blocking temperature distribution was determined from the analysis of the temperature dependence of the coercivity and the ZFC–FC curves. The average blocking temperature was 200 K. Taking into account the width of the distribution of particles over the blocking temperature, it can be concluded that a significant proportion of the nanoparticles have blocking temperatures close to those of use (~300 K). The prepared nanoparticles showed sufficient productivity and high speed in the isolation of DNA from blood.

Funding This work was supported by Russian Foundation for Basic Research, Government of Krasnoyarsk Territory, Krasnoyarsk Region Science and Technology Support Fund, with research projects no. 20–42–242902. We are grateful to the Center of Collective Use of FRC KSC SB RAS for the provided equipment.

References

- Kudr, J., Haddad, Y., Richtera, L., Heger, Z., Cernak, M., Adam, V., Zitka, O.: Magnetic nanoparticles: from design and synthesis to real world applications. *Nanomaterials* **7**, 243 (2017). <https://doi.org/10.3390/nano7090243>
- Tartaj, P., Morales, M. a del P., Veintemillas-Verdaguer, S., Gonz lez-Carre o, T., Serna, C.J.: The preparation of magnetic nanoparticles for applications in biomedicine. *J. Phys. D. Appl. Phys.* **36**, R182–R197 (2003). <https://doi.org/10.1088/0022-3727/36/13/202>
- Komina, A.V., Yaroslavtsev, R.N., Gerasimova, Y.V., Stolyar, S.V., Olkhovsky, I.A., Bairmani, M.S.: Magnetic nanoparticles for extracting DNA from blood cells. *Bull. Russ. Acad. Sci. Phys.* **84**, 1362–1365 (2020). <https://doi.org/10.3103/S1062873820110155>
- Tang, C., He, Z., Liu, H., Xu, Y., Huang, H., Yang, G., Xiao, Z., Li, S., Liu, H., Deng, Y., Chen, Z., Chen, H., He, N.: Application of magnetic nanoparticles in nucleic acid detection. *J. Nanobiotechnology*. **18**, 62 (2020). <https://doi.org/10.1186/s12951-020-00613-6>
- Wang, J., Ali, Z., Si, J., Wang, N., He, N., Li, Z.: Simultaneous extraction of DNA and RNA from hepatocellular carcinoma (Hep G2) based on silica-coated magnetic nanoparticles. *J. Nanosci. Nanotechnol.* **17**, 802–806 (2017). <https://doi.org/10.1166/jnn.2017.12442>
- Stolyar, S.V., Krasitskaya, V.V., Frank, L.A., Yaroslavtsev, R.N., Chekanova, L.A., Gerasimova, Y.V., Volochaev, M.N., Bairmani, M.S., Velikanov, D.A.: Polysaccharide-coated iron oxide nanoparticles: synthesis, properties, surface modification. *Mater. Lett.* **284**, 128920 (2021). <https://doi.org/10.1016/j.matlet.2020.128920>
- Chen, Z., Wu, Y., Chen, H., Mou, X., Chen, Z., Deng, Y., Liu, B., Wan, S.: Design and application of automatic and rapid nucleic acid extractor using magnetic nanoparticles. *J. Nanosci. Nanotechnol.* **16**, 6998–7004 (2016). <https://doi.org/10.1166/jnn.2016.12702>
- Wu, Y., Chen, H., Chen, Z., Nie, L., Liu, B., He, N.: Multifunctional device for nucleic acid extraction based on magnetic separation and its co-working with liquid handling system for high throughput sample preparation. *J. Nanosci. Nanotechnol.* **16**, 6919–6924 (2016). <https://doi.org/10.1166/jnn.2016.12583>
- Dadfar, S.M., Roemhild, K., Drude, N.I., von Stillfried, S., Knüchel, R., Kiessling, F., Lammers, T.: Iron oxide nanoparticles: diagnostic, therapeutic and theranostic applications. *Adv. Drug Deliv. Rev.* **138**, 302–325 (2019). <https://doi.org/10.1016/j.addr.2019.01.005>
- Chilom, C.G., Sandu, N., Bălăsoiu, M., Yaroslavtsev, R.N., Stolyar, S.V., Rogachev, A.V.: Ferrihydrite nanoparticles insights: structural characterization, lactate dehydrogenase binding and virtual screening assay. *Int. J. Biol. Macromol.* **164**, 3559–3567 (2020). <https://doi.org/10.1016/j.ijbiomac.2020.08.242>
- Stolyar, S.V., Balaev, D.A., Ladygina, V.P., Dubrovskiy, A.A., Krasikov, A.A., Popkov, S.I., Bayukov, O.A., Knyazev, Y.V., Yaroslavtsev, R.N., Volochaev, M.N., Iskhakov, R.S., Dobretsov, K.G., Morozov, E.V., Falaleev, O.V., Inzhevatin, E.V., Kolenchukova, O.A., Chizhova, I.A.: Bacterial ferrihydrite nanoparticles: preparation, magnetic properties, and application in medicine. *J. Supercond. Nov. Magn.* **31**, 2297–2304 (2018). <https://doi.org/10.1007/s10948-018-4700-1>
- Borlido, L., Azevedo, A.M., Roque, A.C.A., Aires-Barros, M.R.: Magnetic separations in biotechnology. *Biotechnol. Adv.* **31**, 1374–1385 (2013). <https://doi.org/10.1016/j.biotechadv.2013.05.009>
- Concas, G., Congiu, F., Muscas, G., Peddis, D.: Determination of blocking temperature in magnetization and Mössbauer time scale: a functional form approach. *J. Phys. Chem. C*. **121**, 16541–16548 (2017). <https://doi.org/10.1021/acs.jpcc.7b01748>
- Wickman, H.H., Klein, M.P., Shirley, D.A.: Paramagnetic hyperfine structure and relaxation effects in Mössbauer spectra: Fe57 in ferrichrome A. *Phys. Rev.* **152**, 345–357 (1966). <https://doi.org/10.1103/PhysRev.152.345>
- van der Woude, F., Dekker, A.J.: The relation between magnetic properties and the shape of Mössbauer spectra. *Phys. status solidi.* **9**, 775–786 (1965). <https://doi.org/10.1002/pssb.19650090314>
- Iskhakov, R.S., Komogortsev, S.V., Stolyar, S.V., Prokof'ev, D.E., Zhigalov, V.S.: Structure and magnetic properties of nanocrystalline condensates of iron obtained by pulse plasma evaporation. *Phys. Met. Metallogr.* **88**, 261–269 (1999)

17. Komogortsev, S.V., Iskhakov, R.S., Balaev, A.D., Okotrub, A.V., Kudashov, A.G., Momot, N.A., Smirnov, S.I.: Influence of the inhomogeneity of local magnetic parameters on the curves of magnetization in an ensemble of Fe₃C ferromagnetic nanoparticles encapsulated in carbon nanotubes. *Phys. Solid State*. **51**, 2286–2291 (2009). <https://doi.org/10.1134/S1063783409110158>
18. Komogortsev, S.V., Iskhakov, R.S., Balaev, A.D., Kudashov, A.G., Okotrub, A.V., Smirnov, S.I.: Magnetic properties of Fe₃C ferromagnetic nanoparticles encapsulated in carbon nanotubes. *Phys. Solid State*. **49**, 734–738 (2007). <https://doi.org/10.1134/S1063783407040233>
19. Pfeiffer, H.: Determination of anisotropy field distribution in particle assemblies taking into account thermal fluctuations. *Phys. status solidi*. **118**, 295–306 (1990). <https://doi.org/10.1002/pssa.2211180133>
20. Sharrock, M.P.: Time dependence of switching fields in magnetic recording media (invited). *J. Appl. Phys.* **76**, 6413 (1994). <https://doi.org/10.1063/1.358282>
21. Usov, N.A., Grebenshchikov, Y.B.: Hysteresis loops of an assembly of superparamagnetic nanoparticles with uniaxial anisotropy. *J. Appl. Phys.* **106**, 023917 (2009). <https://doi.org/10.1063/1.3173280>
22. Poperechny, I.S., Raikher, Y.L., Stepanov, V.I.: Dynamic hysteresis of a uniaxial superparamagnet: semi-adiabatic approximation. *Phys. B Condens. Matter*. **435**, 58–61 (2014). <https://doi.org/10.1016/j.physb.2013.08.049>
23. García-Otero, J., García-Bastida, A., Rivas, J.: Influence of temperature on the coercive field of non-interacting fine magnetic particles. *J. Magn. Magn. Mater.* **189**, 377–383 (1998). [https://doi.org/10.1016/S0304-8853\(98\)00243-1](https://doi.org/10.1016/S0304-8853(98)00243-1)
24. Knyazev, Y. V., Balaev, D.A., Kirillov, V.L., Bayukov, O.A., Mart'yanov, O.N.: Mössbauer spectroscopy study of the superparamagnetism of ultrasmall ε-Fe₂O₃ nanoparticles. *JETP Lett.* **108**, 527–531 (2018). <https://doi.org/10.1134/S0021364018200092>
25. Tronc, E., Chanéac, C., Jolivet, J.P.: Structural and magnetic characterization of ε-Fe₂O₃. *J. Solid State Chem.* **139**, 93–104 (1998). <https://doi.org/10.1006/jssc.1998.7817>
26. Denardin, J.C., Brandl, A.L., Knobel, M., Panissod, P., Pakhomov, A.B., Liu, H., Zhang, X.X.: Thermoremanence and zero-field-cooled/field-cooled magnetization study of Cox(SiO₂)_{1-x} granular films. *Phys. Rev. B*. **65**, 064422 (2002). <https://doi.org/10.1103/PhysRevB.65.064422>
27. Tobia, D., Winkler, E., Zysler, R.D., Granada, M., Troiani, H.E., Fiorani, D.: Exchange bias of Co nanoparticles embedded in Cr₂O₃ and Al₂O₃ matrices. *J. Appl. Phys.* **106**, 103920 (2009). <https://doi.org/10.1063/1.3259425>
28. Balaev, D.A., Krasikov, A.A., Dubrovskiy, A.A., Popkov, S.I., Stolyar, S.V., Bayukov, O.A., Iskhakov, R.S., Ladygina, V.P., Yaroslavtsev, R.N.: Magnetic properties of heat treated bacterial ferrihydrite nanoparticles. *J. Magn. Magn. Mater.* **410**, 171–180 (2016). <https://doi.org/10.1016/j.jmmm.2016.02.059>
29. Raikher, Y.L., Stepanov, V.I.: Thermal fluctuation effect on the ferromagnetic-resonance line-shape in disperse ferromagnets. *JETP*. **102**, 1409–1423 (1992)
30. Poperechny, I.S., Raikher, Y.L.: Ferromagnetic resonance in uniaxial superparamagnetic particles. *Phys. Rev. B*. **93**, 014441 (2016). <https://doi.org/10.1103/PhysRevB.93.014441>
31. Pisane, K.L., Despeaux, E.C., Seehra, M.S.: Magnetic relaxation and correlating effective magnetic moment with particle size distribution in maghemite nanoparticles. *J. Magn. Magn. Mater.* **384**, 148–154 (2015). <https://doi.org/10.1016/j.jmmm.2015.02.038>
32. Gazeau, F., Shilov, V., Bacri, J.C., Dubois, E., Gendron, F., Perzynski, R., Raikher, Y.L., Stepanov, V.I.: Magnetic resonance of nanoparticles in a ferrofluid: evidence of thermofluctuational effects. *J. Magn. Magn. Mater.* **202**, 535–546 (1999). [https://doi.org/10.1016/S0304-8853\(99\)00156-0](https://doi.org/10.1016/S0304-8853(99)00156-0)
33. Pérez, N., Guardia, P., Roca, A.G., Morales, M.P., Serna, C.J., Iglesias, O., Bartolomé, F., García, L.M., Batlle, X., Labarta, A.: Surface anisotropy broadening of the energy barrier distribution in magnetic nanoparticles. *Nanotechnology* **19**, 475704 (2008). <https://doi.org/10.1088/0957-4484/19/47/475704>

Publisher's Note Springer Nature remains neutral with regard to jurisdictional claims in published maps and institutional affiliations.